

# RF BEAM DEFLECTORS FOR CTF3 COMBINER RING

D. Alesini, R. Boni, A. Gallo, F. Marcellini, LNF-INFN, Frascati, Rome, Italy  
 A. Kucharczyk, S. Kulinski, M. Pachan, E. Plawski,  
 The Andrzej Soltan Institute for Nuclear Studies, Otwock-Swierk, Poland

## Abstract

An important goal of the CLIC Test Facility CTF3 project, presently on its preliminary phase at CERN, is to verify the feasibility of bunch interlacing for the generation of 30 GHz RF power, by increasing the bunch frequency of the drive beam. Two RF deflectors are foreseen to inject in a Combiner Ring. This paper presents their design and fabrication issues.

## 1 INTRODUCTION

The bunch train compression scheme for CLIC test Facility CTF3 [1] relies on the feasibility of fast RF deflectors. The beam dynamics in the combiner ring and, in particular, the effects of the beam loading in the RF deflectors have been carefully investigated [2,3]. The simulation results indicate that a pair of CERN RF separators [4] (the so-called *Langelier structures*) used as RF deflectors does not degrade significantly the quality of the beam extracted from the combiner ring. The main parameters of the Langelier structure used as CTF3 RF deflectors are summarized in Table 1.

In the following we report the design procedure and the mechanical fabrication techniques followed to construct the two deflectors.

Table 1: CTF3 RF Deflector parameters.

Nom. Energy $E_n$	150 [MeV]
Max Energy $E_{max}$	300 [MeV]
Frequency $f$	2.99855 [GHz]
Number of cell	10
De-phasing/cell	$2\pi/3$
Cell length $d$	33.33 [cm]
Group velocity $v_g/c$	-0.0244
Phase velocity $v_{ph}/c$	1
RF power $P_{RF}$	$\sim 1.5$ [MW] (@ $E_n$ ) $\sim 6$ [MW] (@ $E_{max}$ )
Deflection $\phi$	5 [mrad]
$R/Q = v_g/\omega \cdot (F_{\perp}/e)^2/P_{RF}$	1380 [ $\Omega/m$ ]

## 2 MAFIA AND HFSS SIMULATIONS RESULTS

The design of the RF deflectors has been done scaling to the CTF3 working frequency (2.99855 GHz) the dimensions of CERN RF separators with a reduced number of cells. These are disk-loaded backward

waveguides working in the  $2\pi/3$   $EH_{11}$  hybrid mode [5] already optimized [6] for beam deflection. The final 10 cells structure is sketched in Fig. 1.

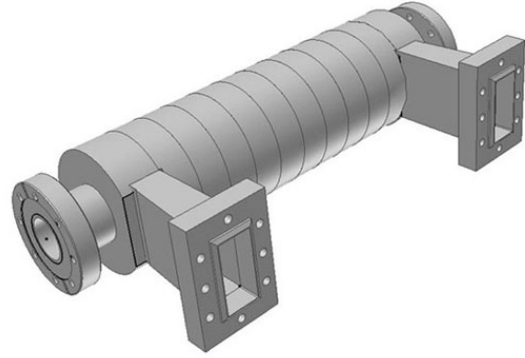


Figure 1: Sketch of the RF deflector.

### 2.1 Single Cell Simulations

With the electromagnetic code MAFIA [7] we have simulated the scaled single cell (Fig. 2) and we have computed the local sensitivity of the  $2\pi/3$  mode frequency with respect to the variation of each cell dimension (Table 2).

Table 2: local sensitivity of the deflecting mode frequency vs. cell dimensions

Dimension	Sensitivity
a	$\partial f/\partial a = -13.2$ MHz/mm
b	$\partial f/\partial b = -49.7$ MHz/mm
c	$\partial f/\partial t = 2.9$ MHz/mm
d	$\partial f/\partial d = 1.2$ MHz/mm

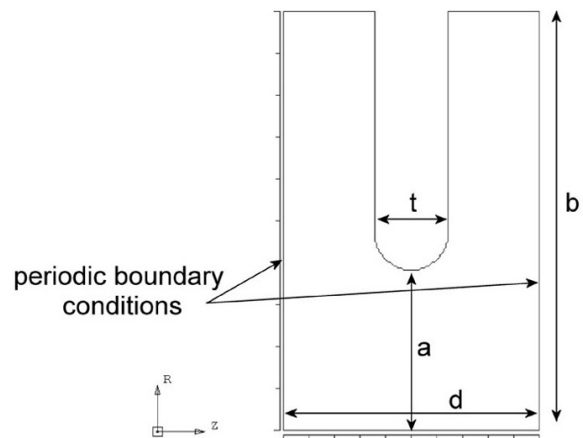


Figure 2: Sketch of the single cell 2D profile.

The  $2\pi/3$   $EH_{11}$  mode can degenerate in 2 frequencies of orthogonal polarity. The vertical one has been shifted far enough from the operating mode (horizontal polarity) in order to avoid excitation by the RF generator or the beam itself. This has been achieved by means of 2 longitudinal rods crossing off-axis the cells (just like the CERN separators) as shown in Fig. 3.

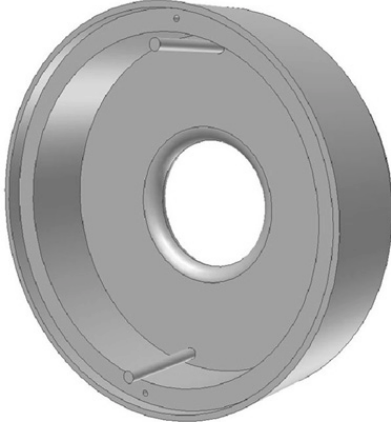


Figure 3: Sketch of the single cell 3D profile.

The frequency shift of both polarities, caused by the break of the azimuthal symmetry due to the rods, has been calculated with the code HFSS [8]. We obtained a shift of ~50 MHz for the vertical polarity and a negligible shift of the horizontal operating mode (~80 kHz).

We have, finally, calculated the  $2\pi/3$  mode frequency of the single cell with rods considering also the problem of faceting in HFSS. In fact the code uses a regular polygon to model a circle or an arc and, depending on the starting vector for faceting, the polygon can be entirely inside or outside the arc to be modeled. In order to control the systematic error due to faceting, in the final single cell simulations we have considered the radius of curvature properly corrected in order to have the corresponding polygon areas equal to those of the ideal circles. The final dimensions of the single cell are reported in Table 3 with the  $2\pi/3$  mode frequencies obtained by HFSS (3D cell with rods) and by MAFIA (2D cell without rods).

The dispersion curve of the deflecting mode obtained by MAFIA is plotted in Fig. 4.

Table 3: Final dimensions of the cell and RF deflectors parameters.

Final dimensions of the cells	$a = 21.43$ mm
	$b = 56.01$ mm
	$d = 33.33$ mm
	$t = 9.53$ mm
RF deflector parameters (HFSS and MAFIA)	$f=2.9986$ [GHz] (MAFIA)
	$f=2.9983$ [GHz] (HFSS)
	$v_g=-0.0237*c$ (MAFIA)
	$R/Q=1460$ [ $\Omega/m$ ] (HFSS)

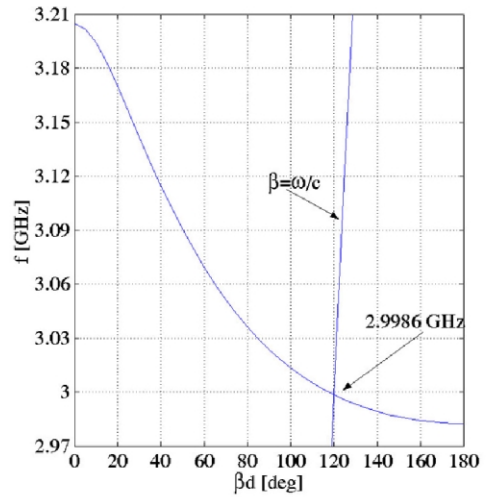


Figure 4: Dispersion curve of the deflecting mode obtained by MAFIA.

## 2.2 Complete Structure Simulations

In order to evaluate the coupler efficiency we have simulated with HFSS the structure with the proper boundary conditions and port excitation.

The obtained reflection coefficient ( $S_{11}$ ) at the device input port is plotted versus frequency in Fig. 5. It is evident that, at the working frequency 2.99855 GHz, just few percent of the input power is reflected.

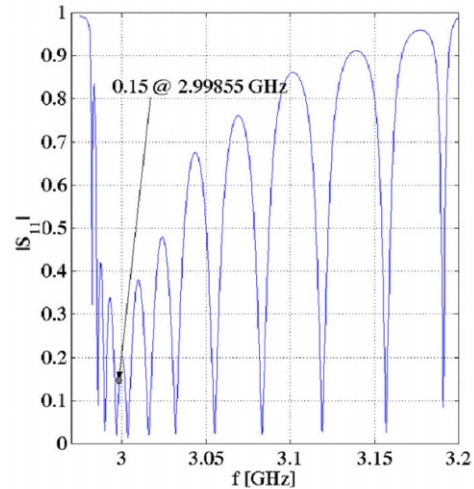


Figure 5: Reflection coefficient at the input port of the deflector as a function of frequency.

## 3 MECHANICAL FABRICATION TECHNIQUE

The deflectors are made of OFHC high quality copper using hard soldering (brazing) technique well mastered in production processes of accelerating structures in S band. Soldering is done in steps, in hydrogen atmosphere. Unlike the old CERN procedure, the single cells of deflector are designed and produced in the form of cups (Figure 3) reducing the number of soldered joints by a factor 2.

Before the production of the final deflectors an aluminium full-scale prototype (shown Fig. 6) has been fabricated in order to verify the validity of the performed calculations. The measurements (single cell resonant frequency, dispersion curve) have confirmed the simulation results for the two different polarities.

The deflector components are fabricated with the aid of numerical lathe and milling machines. A three steps soldering (890-780-680 °C) procedure is applied to join the deflector components. Intermediate measurements (single cell frequencies and dispersion curves before and after soldering) made on prototypes copper cells and final structures have been performed in order to control the frequencies of the cells and the changes introduced by the soldering procedure.

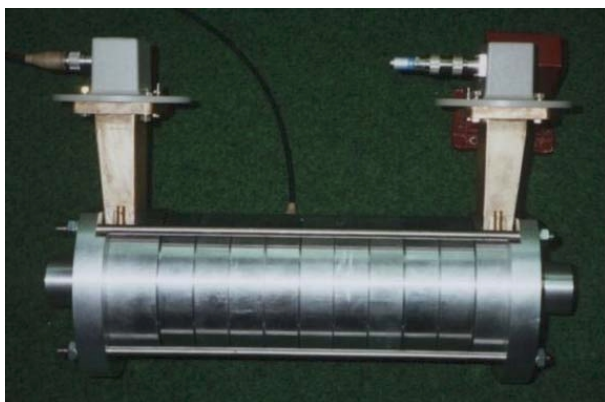


Figure 6: Aluminium prototype.

#### 4 FINAL TUNING AND MEASUREMENTS

A dedicated test set was constructed to check the frequency of each cell before soldering. The frequencies of the first two monopoles and dipoles were measured and compared with those obtain by HFSS simulations. The frequency deviations due to the presence of measuring antennas and to the cell actual temperature were taken into account. The comparison of the calculated and measured frequencies in a sample of 8 cells is reported in Table 4.

Table 4. Comparison of calculated and measured frequencies of the cells before soldering

		Mono 0	Mono $\pi$	Dipole $\pi$	Dipole 0
		MHz	MHz	MHz	MHz
HFSS		2105.7	2176.8	3010.9	3226.0
		Measured frequency deviation [MHz]			
Cell Number	1	-0.295	-0.674	0.096	-0.846
	2	-0.395	-0.599	-0.179	-0.846
	3	-0.325	-0.549	-0.079	-0.771
	4	-0.435	-0.675	-0.189	-0.926
	5	-0.375	-0.535	-0.264	-0.840
	6	-0.335	-0.594	-0.044	-0.826
	7	-0.335	-0.554	-0.104	-0.825
	8	-0.295	-0.534	-0.104	-0.826

The measured dispersion curve of a stack of 8 cells (+2 half cells) before soldering is shown in Fig. 7 and is in a very good agreement with the simulations results.

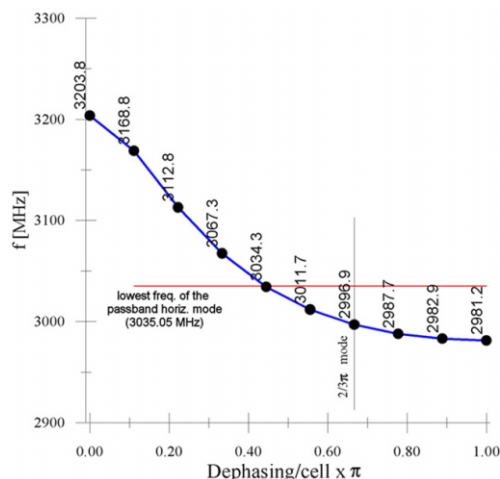


Figure 7: Dispersion curve of the defl. mode measured in air at 24.5 °C with 8 cells (+2 half cells) before soldering.

To evaluate the effect of soldering, a series of 4 pilot copper cells was measured before and after soldering. The results are shown in Table 5. Being the deflector relatively short the effect of soldering is quite negligible and, anyway, can be taken into account.

Table 5: Resonant frequencies of an assembling of 4 pilot copper cells before and after soldering.

Mode	Freq. before solder [MHz]	Freq. after solder [MHz]	$\Delta f$ [kHz]
1	2986.180	2986.006	-174
2	3002.830	3002.484	-346
3	3043.374	3943.177	-197
4	3126.250	3126.030	-220
5	3211.924	3211.582	-342

#### 5 CONCLUSIONS AND ACKNOWLEDGEMENT

The first deflector is almost ready for shipment to LNF for vacuum tests. It will be installed within June 2002 in the EPA ring for the CTF3 preliminary phase. the second deflector will be ready within July 2002. The authors warmly thank Mr. G. Fontana for the fruitful collaboration in the mechanical design of the deflectors.

#### 6 REFERENCES

- [1] H. H. Braun et al., CERN 99-06, 1999
- [2] A. Gallo et al., proc. of EPAC 2000 Conf., p. 465
- [3] D. Alesini et al., CTFF3-003, 2001
- [4] D. Alesini, CTFF3-007, 2002
- [5] Ph. Bernard et al., CERN 68-30, 1968
- [6] Y. Garault, CERN 64-43, 1964
- [7] Ph. Bernard et al., CERN 70-26
- [8] <http://www.cst.de>
- [9] <http://www.ansoft.com/home2.cfm>